Dalton Transactions

Accepted Manuscript

ROYAL SOCIETY OF CHEMISTRY

www.rsc.org/dalton

Journal Name

RSCPublishing

ARTICLE

A new TPE-based tetrapodal ligand and its Ln(III) complexes: Multi-stimuli responsive AIE (aggregation-induced emission)/ILCT(intraligand charge transfer)-Bifunctional Photoluminescence and NIR emission sensitization

Cite this: DOI: 10.1039/xoxxooooox

Received ooth January 2012,
Accepted ooth January 2012

DOI: 10.1039/xoxxooooox

www.rsc.org/

Yi-Xuan Zhu[a], Zhang-Wen Wei[a], Mei Pan[a,b]*, Hai-Ping Wang[a], Jian-Yong Zhang[a], and Cheng-Yong Su[a,c]*

Tetrapodal zwitterionic-type ligand featuring both AIE (aggregation-induced emission) and ILCT (intraligand charge transfer) properties, namely 1,1',1'',1'''-(4,4',4'',4'''-(ethene-1,1,2,2-tetrayl)tetrakis(benzene-4,1-diyl))tetrakis(methylene)tetrapyridin-4(1*H*)-one (TPE-4PO) has been designed and applied to the assembly of lanthanide complexes LIFM-21(Ln) (Ln = Sm, Eu, Gd, Tb and Dy). Apart from sensitization of NIR emission of Sm^{3+} and Dy^{3+}, the resulting ligand and lanthanide complexes show both AIE and ILCT-related photoluminescent behaviors. The photo-response of this system to different aggregation states, solvents' polarity and mechanical grinding was demonstrated by distinguishable emission intensities and colours.

Introduction

AIE (Aggregation Induced Emission) has aroused great attention in recent years, and is finding potential applications in chemical sensors, bio-probes and imaging labels, organic light emitting devices (OLED), and so on.[1-3] Among which, tetraphenylethylene (TPE) based molecules are most intensively studied, which show aggregation-enhanced photoluminescence compared with their basically non-luminescent or weakly luminescent solution state.[4,5] The mechanism is often related with the rigidity of C-C single bonds on the backbone of TPE in aggregated system, which are freely rotatable in the solution state and will bring photoluminescence quenching due to nonradiative transitions.[6] Simultaneously, some TPE-based AIE molecules also perform solid state mechanochromism, in which the materials can emit photoluminescence with different colors upon mechanical forces,[7,8] and therefore, can find wide applications in sensors,[9] memory chips[10] and anti-counterfeiting labels.[11] However, the inherent reasons for such mechano-fluorochromism are still not clear, although the phase transition from crystalline to amorphous state is generally believed to have some effects.[12,13] On the other hand, organic ligands having ILCT (intraligand charge transfer) potentials tend to perform specific photophysical and photochemical properties, such as large Stokes shift, solvent-responsive emission, and so on, and are also attracting great attention in fabricating novel photoluminescent materials with good performance. In our earlier reports, we have designed a series of zwitterionic type ILCT ligands showing versatile absorption bands and very wide excited states comprising both ILCT and ligand-based singlet/triplet states. Therefore, highly efficient visible and NIR emissions of the whole Ln^{3+} series can be sensitized by these ligands, and meanwhile, tunable color and single phase white light emission can also be easily achieved in the afforded lanthanide complexes.[14-17] Combining the above two factors together, we anticipate a new class of AIE/ILCT bi-functional luminescent molecules, whose photoluminescence can be stimulated by multiple external environments, including aggregation states, mechanical forces, solvent polarities. Simultaneously, these molecules can also serve as efficient antenna to sensitize the emission of lanthanide ions. Furthermore, these combined properties can be integrated into the fabrication of various kinds of novel assemblies, such as macromolecule polymers, organo-inorganic hybrid materials, metal-organic coordination supramolecules, and so on, bringing specifically attractive photochemical and photophysical properties.[18,19] However, up to now, such kinds of explorations are still quite limited.

Herein, we report a new tetrapodal organic ligand (TPE-4PO) comprising both AIE and ILCT components and characters, which is further applied to coordinate with Ln(III) ions. Combined multi-stimuli responsive AIE/ILCT-related visible emission and highly ligand-sensitized Ln(III)-NIR emission are observed in this new type of organic ligand and its lanthanide coordination polymers.

Experimental

Materials and methods

All the experimental materials were of AR grade and used as purchased without further purification. The C, H, N elemental analyses were measured on a Perkin-Elmer 240 elemental analyzer. ^{1}H NMR spectra were recorded on Bruker Avance III 400 NMR spectrometer using TMS as the internal standard. TGA curves were performed on a NETZSCH TG 209 instrument in N_2 atmosphere with a heating rate of 10 ^{o}C min^{-1}. IR spectra were measured on a Nicolet 205 FT-IR spectrometer with KBr pellets (400−4000 cm^{-1}). Powder X-ray diffraction (PXRD) data were recorded on a Rigaku SmartLab X-ray powder diffractometer (Cu-Kα, λ = 1.54056 Å). UV-Vis absorption spectra were recorded using a Shimadzu UV-250PC spectrophotometer. Photoluminescence spectra and photophysical data were measured on EDINBURGH FLS980 spectrophotometer. The absolute quantum yield measurements for the visible emission (400 to 800 nm) were performed in a quartz sample holder using an integrating sphere attached to the equipment. The overall quantum yield $\Phi_{overall}$ is calculated by

$$\Phi_{\text{overall}} = \frac{\text{S(Em)}}{\text{S(Abs)}} = \frac{\int \frac{\lambda}{hc}\left[I_{em}^{sample}(\lambda) - I_{em}^{reference}(\lambda)\right]d\lambda}{\int \frac{\lambda}{hc}\left[I_{ex}^{reference}(\lambda) - I_{ex}^{sample}(\lambda)\right]d\lambda} \qquad (1)$$

where S(Abs) is the number of photons absorbed by the sample and S(Em) is the number of photons emitted from the sample, λ is the wavelength, h is Planck's constant, c is the velocity of light, $I_{sample\ (ex)}$ and $I_{reference\ (ex)}$ are the integrated intensities of the excitation light with and without a sample, $I_{sample\ (em)}$ and $I_{reference\ (em)}$ are the photoluminescence intensities with and without the sample, respectively.

Crystallography

The single-crystal diffraction data of Tb(III) coordination complex from TPE-4PO (LIFM-21(Tb)) were collected on an Agilent SuperNova diffractometer with the Enhance X-ray Source of Cu-Kα radiation (λ = 1.54184 Å) at 173 K. Absorption corrections were applied using multiscan technique. The structure of the coordination complex was solved by direct method of SHELXS and refined against F^2 using the SHELXL programs.[20] All the non-hydrogen atoms were treated with anisotropic parameters. The crystallographic data and structural refinement information for the complex are listed in Table S1, and the selected bond lengths and bond angles listed in Table S2. Crystallographic data for the structure have been deposited with the Cambridge Crystallographic Data Centre as supplementary publication no. CCDC 1425305.

Computational methodology

DFT theoretical calculations were performed with Gaussian 09 software to optimize the ground state geometrical configuration of TPE-4PO ligand applying B3LYP method (6-31G* basis set for atoms C, H, O, and N).

Synthesis of the ligand

1,1',1'',1'''-(4,4',4'',4'''-(ethene-1,1,2,2-tetrayl)tetrakis(benzene-4,1-diyl))tetrakis(methylene)tetrapyridin-4(1*H*)-one (TPE-4PO):

Peparation of **2** (1,1,2,2-tetrap-tolylethene): 1,1,2,2-tetra*p*-tolylethene was synthesized according to a modified literature method[21]: Zinc powder (1.0 g, 15.3 mmol) was added into a 100 mL double-neck flask. Under N_2 atmosphere, 25 mL dry THF was added, which was cooled to -10 ^{o}C, and then $TiCl_4$ (1.1 mL, 10 mmol) and pyridine (0.05 mL, 0.6 mmol) were added dropwisely. The mixture was refluxed at 85 ^{o}C for 2 hours, cooled to 0 ^{o}C, and 20 mL THF solution of di-*p*-tolylmethanone (**1**, 1.05 g, 5 mmol) was added. The solution was stirred at room temperature for 10 minutes and further refluxed at 85 ^{o}C for 12 hours. Upon completion of the reaction, the solution was cooled to room temperature and poured into 40 mL 40% water solution of K_2CO_3, which was stirred strongly for 5 minutes and then filtered. The filtrate was substracted with CH_2Cl_2, washed successively with water, brine, and dried with $MgSO_4$. Light yellow solid was obtained by rotary evaporation, and purified by column chromatography (silica gel, petroleum ether) to result in white product of **2**. Yield, 89%. ^{1}H NMR (400 MHz, $CDCl_3$, 25 °C): δ 6.92 (s, 16H), 2.28 (s, 12H).

Peparation of **3** (1,1,2,2-tetra-*kis*(4-(bromomethyl)phenyl)ethene): 388.54 mg (1 mmol) 1,1,2,2-tetra*p*-tolylethene (**2**) obtained in the previous step was added into a 50 mL round bottom flask, and then NBS (711.96 mg, 4 mmol), AIBN (15 mg), benzene (15 mL) were added. The mixture was reacted at 85 ^{o}C for 3 hours, cooled to room temperature, and filtered. The clear filtrate was evaporated to get yellow solid, which was purified by column chromatography (silica gel, ethyl acetate/petroleum ether, v:v=1:15) to result in pale yellow product of **3**. Yield, 61%. ^{1}H NMR (400 MHz, $CDCl_3$, 25 °C): δ 7.21-7.12 (m, 8H), 6.98 (d, J = 8.2 Hz, 8H), 4.45 (s, 8H).

Peparation of **TPE-4PO**: A mixture of 4-hydroxypyridine (125.5 mg, 1.32 mmol) and K_2CO_3 (331.7 mg, 2.4 mmol) was refluxed in ethanol (15 ml) at 95 ^{o}C for 4 hours, and then 1,1,2,2-tetra-*kis*(4-(bromomethyl)phenyl)ethene (**3**, 211.2 mg, 0.3 mmol) was added. The mixture was further refluxed at 95 °C for 48 h and then filtered. The filtrate was evaporated to get brown solid, which was purified by column chromatography (silica gel, MeOH) to result in the final pale yellow product of TPE-4PO. Yield: 55%. ^{1}H NMR (400 MHz, CD_3OD, 25 °C): δ 7.82 (d, J = 7.5 Hz, 8H), 7.06 (dd, J = 19.7, 8.3 Hz, 16H), 6.46 (d, J = 7.5 Hz, 8H), 5.08 (s, 8H). ^{13}C NMR (101 MHz, CD_3OD, 25 °C): δ 179.42, 143.41, 141.85, 140.78, 134.35,

131.61, 127.15, 117.20, 59.35 (Fig. S1). IR (cm^{-1}, KBr): 3393.45(m), 1638.70(s), 1544.28(s), 1399.91(m), 1181.13(m), 1114.74(w), 1019.32(w), 854.48(m), 699.37(w).

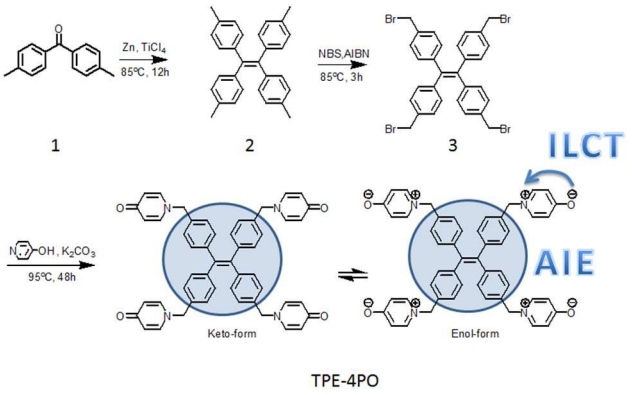

Scheme 1 Synthetic route for the ligand TPE-4PO, showing the tautomeric transition between Keto- and Enol-form, and combination of AIE and ILCT characters.

Syntheses of Ln-complexes

LIFM-21(Tb) – $\{[Tb(TPE\text{-}4PO)(NO_3)_2(H_2O)]\cdot NO_3\cdot 2H_2O\}_n$: A solution of TEP-4PO (11.4 mg, 0.015 mmol) in MeOH (1.5 mL) was added into a solution of $Tb(NO_3)_3\cdot 3H_2O$ (8.0 mg, 0.02 mmol) in acetone (1 ml) at room temperature. A large quantity of white precipitates were resulted, into which 1.5 mL DMF was added under ultra sonification. The white precipitates were dissolved and then filtered. Slow diffusion of acetone into the clear filtrate over 3 days afforded block crystals suitable for X-ray diffraction. Yield: 34-39%. EA for $C_{50}H_{46}N_7O_{16}Tb$: calc. C, 51.78, H, 4.00, N, 8.45%; Found, C, 52.01, H, 3.918, N, 8.38%.

The complexes of Sm, Eu, Gd, and Dy (**LIFM-21(Sm), LIFM-21(Eu), LIFM-21(Gd), LIFM-21(Dy)**) were obtained using the similar procedure. EA for $C_{50}H_{44}N_7O_{15}Sm$ ($\{[Sm(TPE\text{-}4PO)(NO_3)_2(H_2O)]\cdot NO_3\cdot H_2O\}_n$): calc. C, 52.99, H, 3.91, N, 8.65%; Found, C, 52.63, H, 3.825, N, 8.67%. EA for $C_{50}H_{44}N_7O_{15}Eu$ ($\{[Eu(TPE\text{-}4PO)(NO_3)_2(H_2O)]\cdot NO_3\cdot H_2O\}_n$): calc. C, 52.92, H, 3.91, N, 8.64%; Found, C, 52.61, H, 3.926, N, 8.55%. EA for $C_{50}H_{44}N_7O_{15}Gd$ ($\{[Gd(TPE\text{-}4PO)(NO_3)_2(H_2O)]\cdot NO_3\cdot H_2O\}_n$): calc. C, 52.67, H, 3.89, N, 8.60%; Found, C, 52.60, H, 3.913, N, 8.48%. EA for $C_{50}H_{46}N_7O_{16}Dy$ ($\{[Dy(TPE\text{-}4PO)(NO_3)_2(H_2O)]\cdot NO_3\cdot 2H_2O\}_n$): calc. C, 51.71, H, 3.899, N, 8.29%; Found, C, 51.62, H, 3.99, N, 8.43%.

Results and discussion

Structure of TPE-4PO ligand and lanthanide complexes. As shown in Schemes 1 and 2, TPE-4PO possesses both AIE-related tetraphenylethylene core, and charge-separated pyridone ends with ILCT characters. Although we did not get the single crystal of TPE-4PO ligand, its optimized ground state geometry was illustrated by DFT theoretical study. As shown in Fig. 1a, the ligand is stabilized in keto-form on the ground state, with terminal C=O bonds of 1.23-1.24 Å, typical of keto bonding rather than enol one. The HOMO and HOMO-1 orbitals of TPE-4PO are mainly contributed by π orbitals from terminal pyridone rings, and LUMO/LUMO+1 orbitals are comprised of π* orbitals from the central TPE backbone. The energy gap between the HOMO and LUMO orbitals is 0.13 a.u. (3.5 eV). Therefore, ILCT (intraligand charge transfer) can happen between the frontier orbitals of TPE-4PO to result in charge-separated enol-formation.

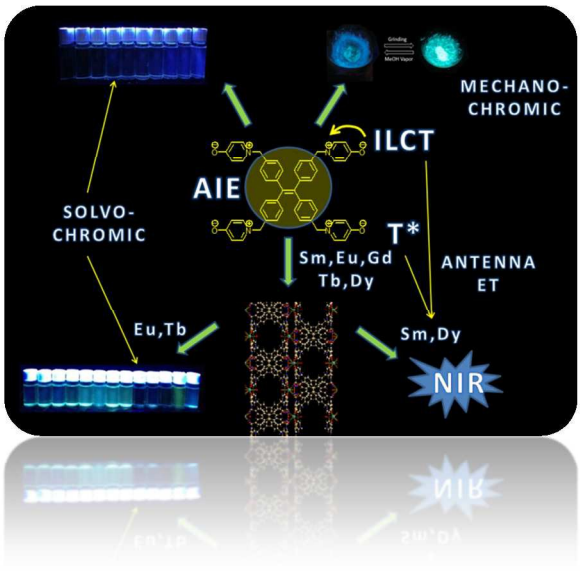

Scheme 2 Multifunctional photoluminecent properties of TPE-4PO ligand and its assembled lanthanide complexes.

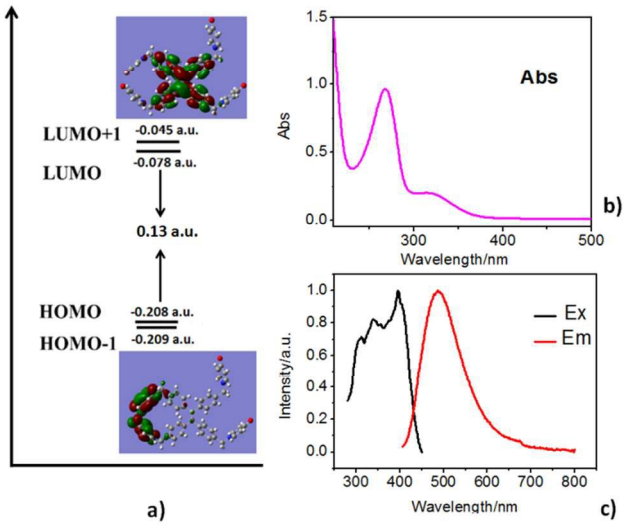

Fig. 1 (a) Diagrams of optimized geometrical structure and frontier orbital energy levels, (b) UV-Vis absorption in ethanol (1×10^{-5} mol L^{-1}), and (c) solid-state photoluminescence spectra (Ex: λ_{em} = 487 nm, Em: λ_{ex} = 397 nm) of TPE-4PO ligand.

UV-Vis absorption (ethanol, 1×10^{-5} mol L^{-1}) and solid state

excitation/emission spectra of TPE-4PO ligand were shown in Figs. 1 b and c. As we can see, TPE-4PO manifests two absorption peaks at 268 and 314 nm in ethanol solution, corresponding to n→π*, π→π* and ILCT transitions in the molecule. Solid state TPE-4PO powder sample represents structured excitation bands from 300 to 450 nm, and shows a broad emission centered at 487 nm by the excitation of 397 nm. The skyish-blue emission of TPE-4PO has a decay lifetime (τ) of 1.76 ns and an absolute quantum yield (Φ) of 28.3%, with CIE coordinate at (0.19, 0.21). The quantum yield of this ligand is comparable to other reported TPE-based molecules.[4,5]

The assembly of TPE-4PO ligand with $Ln(NO_3)_3$ (Ln = Sm, Eu, Gd, Tb, Dy) results in a series of isomorphous lanthanide complexes, LIFM-21(Ln). The solid products of these Ln-complexes are apt to effloresce in air to lose the single crystallinity. However, the powder X-ray diffraction (PXRD) analyses manifest some comparable major peaks, indicating these Ln-complexes form similar coordination frameworks (Fig. S2). We chose LIFM-21(Tb) as a representative to collect the single crystal diffraction data and analyze the crystal structure. LIFM-21(Tb) crystallizes in the orthorhombic *Pban* space group, in which, the extending modes of the TPE-4PO ligand are basically similar to other reported coordination frameworks from TPE-based ligands.[4] However, due to the semi-flexible character of the methylene-linked pyridone ends and the coordination potency of lanthanide ions, the resulted framework structure in LIFM-21(Tb) is unique. In detail, the Tb^{3+} ion is 10-coordinated with four TPE-4PO ligands through terminal pyridone groups, two NO_3^- anions in chelate manner, and two water molecules (Fig. 2a). Each Tb^{3+} ion serves as a four-connecting node, such is also the case with TPE-4PO ligand, linking into a one-dimesional (1D) loop-and-chain structure. In the crystal lattice, such 1D chains are interdigitated in parall to form a 2D layer via π-π interactions (Fig. 2b). The TG curve of complex LIFM-21(Tb) indicates thermal stability up to 400 °C, when the coordination framework starts to collapse (Fig. S3).

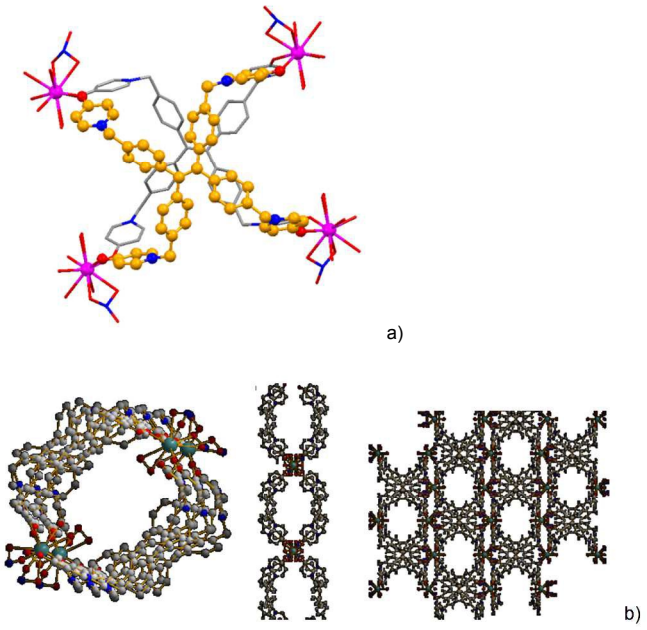

Fig. 2 (a) Crystal structure of LIFM-21(Tb) showing the coordination environment of central Tb^{3+} and TPE-4PO ligands. Pink for Tb, red for O, blue for N, orange and grey for C on two different TPE-4PO ligands. (b) Crystal packing viewed along different directions. The solvent molecules and hydrogen atoms are omitted for clarity.

AIE effect of TPE-4PO ligand. As discussed before, TPE-4PO ligand shows skyish blue emission in the solid state. In order to detect the aggregation effect on the emissive property of the molecule, we dissolve TPE-4PO in good solvent DMSO by adding different ratio of poor solvent CH_2Cl_2. As we can see, when the fraction of CH_2Cl_2 (fw) is lower than 70%, the solution of TPE-4PO is weakly emissive due to the free rotation of C-C single bonds of the four benzyl rings around the ethylene skeleton. The fraction of CH_2Cl_2 higher than 70% results in the aggregation of TPE-4PO molecules in the solution state and leads to abrupt enhancement of its emission, showing obvious AIE effect (Fig. 3). Compared with solid state sample, the emission maximum of TPE-4PO in solution is basically blue-shifted. Furthermore, with the increase of CH_2Cl_2 fraction, the emission profiles become more structured and the resulting CIE coordinates move steadily towards dark blue region. This may be due to the adding of more CH_2Cl_2 results in the weaken of solvent polarity, and the ILCT process of TPE-4PO molecules is restricted to some extent, leading to energy rise of the emission states.[22]

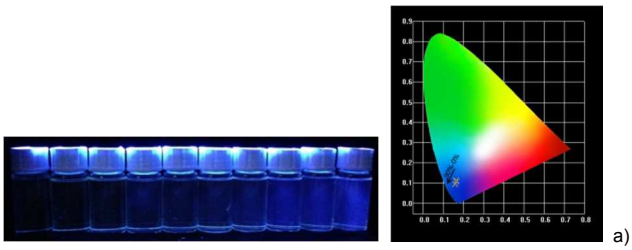

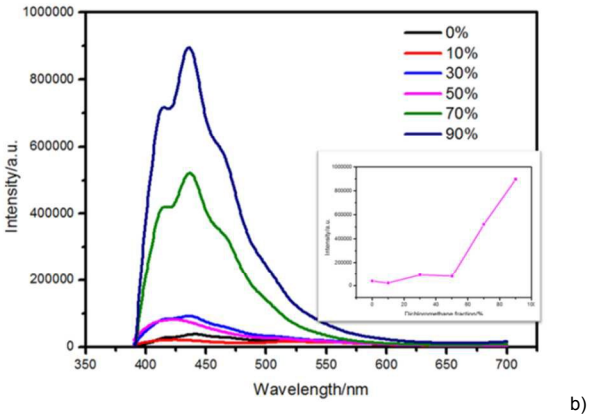

Fig. 3 (a) Fluorescent photographs (left, fw = 0, 10, 20, 30, 40, 50, 60, 70, 80, 90%, from left to right, $c_{TPE-4PO} = 1\times10^{-5}$ mol L^{-1}) and CIE coordinates (right) of TPE-4PO in CH_2Cl_2/DMSO mixtures under 365 nm irradiation. (b) Emission spectra of TPE-4PO in CH_2Cl_2/DMSO mixtures (λ_{ex} = 375 nm), and the inset shows diagram of luminescent intensity vs. CH_2Cl_2 fraction.

TPE-4PO also shows mechanofluorochromic performance, another feature of the AIE-related molecules. As we can see in Fig. 4, the skyish blue fluorescence (0.19, 0.21) of TPE-4PO orginal samples is changed to cyan color (0.20, 0.25) after grinding. Emission spectra (Fig. 4b) manifest the red-shift of the emitting center from 487 to 500 nm. Upon exposure to MeOH (methanol) vapor, the red-shifted fluorescence returns to the original color and this reversible process can be repeated for more than ten cycles (Fig. 4b shows the first five cycles as an example). In order to probe the mechanism of the mechanofluorochromic behavior of TPE-4PO, PXRD were measured for the original and ground/MeOH treated samples. As shown in Fig. 4c, although some diffraction peaks disappear after grinding, we can not detect an obvious transition from crystalline to amorphous state, since the major diffraction peaks still protrude sharply. And upon MeOH vapor-treatment, most of the disappeared peaks are restored. From this result, we propose that the mechanofluorochromic behavior observed in TPE-4PO may be related with the slight changes in packing states of the aggregated molecules before and after grinding/MeOH treatment, instead of the total transition between crystalline and amorphous phases.

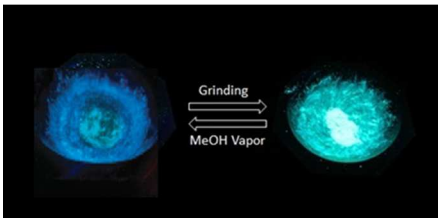

a)

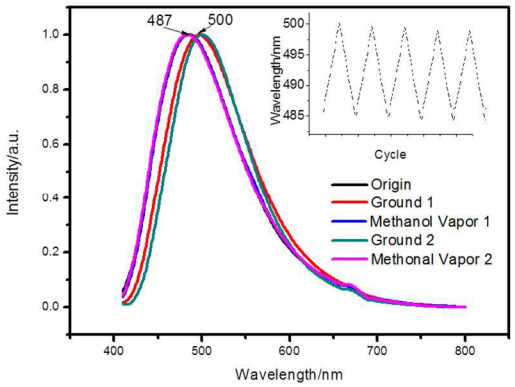

b)

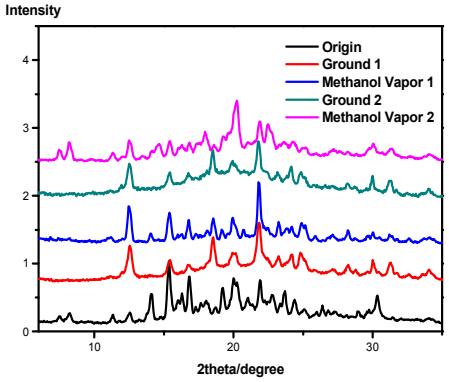

c)

Fig. 4 (a-c) Fluorescent photographs, emission spectra (λ_{ex} = 375 nm), and PXRD patterns of the original, ground and MeOH (methanol) vapor treated TPE-4PO samples.

Antenna effect of TPE-4PO ligand: AIE in visible emitting Eu^{3+}, Tb^{3+} complexes, and sensitized NIR emitting in Sm^{3+}, Dy^{3+} complexes. As a ligand with lower energy ILCT states, TPE-4PO is coordinated with Ln^{3+} ions to explore its sensitization ability for the characteristic lanthanide $f \rightarrow f$ emissions, especially those in the near infrared (NIR) region. Firstly, the phosphorescence spectrum of LIFM-21(Gd) was detected at 77 K to determine the triplet energy level of TPE-4PO. As we can see in Fig. S4, LIFM-21(Gd) manifests broad phosphorescence centered at ~486 nm, therefore, the tripet energy level of TEPE-4PO is estimated to be ~20 576 cm^{-1}. This energy level may be too lower to efficiently sensitize the visible emission of Eu^{3+} ($^5D_0$, 17 277 cm^{-1}) and Tb^{3+} ($^5D_4$, 21 000 cm^{-1}).[23] However, it can be applied for the sensitization of NIR emissions of Sm^{3+} and Dy^{3+} in this series of complexes.

As expected, LIFM-21(Eu) and LIFM-21(Tb) present mainly the blue emission of the ligand TPE-4PO, rather than the characteristic red and green emission of Eu^{3+} and Tb^{3+}. However, after lanthanide coordination, the quantum yield of the blue emission from TPE-4PO in LIFM-21(Tb) is obviously increased, reaching 45.6%. This may be partly due to the further solidification of the C-C single bonds after coordination, and represents another manifestation of AIE phenomenon.[24] Differently, apart from the major broad emission from TPE-4PO ligand, there are also some weak emissions from Eu^{3+} appearing in LIFM-21(Eu), and the total quantum yield in the range 400-800 nm is 10.2%, lower than that of the pure ligand. This shows that there is partly energy transfer happened from TPE-4PO to Eu^{3+} (the triplet energy level of TPE-4PO is higher than the accepting level of Eu^{3+}, so the energy transfer can happen), but the efficiency is not good enough. This may be firstly due to the triplet-metal emitting level mismatch in the energy state, and secondly, we can see there are water molecules directly connected to the lanthanide ions' first coordination sphere, and this may lead to nonradiative energy dissipation progress to quench the luminescence. For LIFM-21(Sm) and LIFM-21(Dy), the luminescence spectrum in visible region is also dominated by ligand-based broad emission (Fig. S5), except that several small peaks relating to Sm^{3+} $^4G_{5/2} \rightarrow {}^6H_{5/2,\ 7/2,\ 9/2}$ emissions can also be observed for LIFM-21(Sm). In comparison, sensitized NIR emission characteristic of lanthanide $f \rightarrow f$ transitions can be detected clearly in these two complexes. For LIFM-21(Sm), the NIR emissions at 902, 944, 1070, and 1190 nm can be assigned to $^4G_{5/2} \rightarrow {}^6F_J$ transitions (J = 3/2, 5/2, 7/2, and 9/2, respectively) of Sm^{3+}. While for LIFM-21(Dy), NIR emission peaks are observed at 940 nm, which is corresponding to the $^4F_{9/2} \rightarrow {}^6H_{5/2}$ transition of Dy^{3+}. The decay lifetime for the NIR emission in these two lanthanide complexes are 26 μs (944 nm, $^4G_{5/2}$ for Sm^{3+}) and 5.2 μs ($^4F_{9/2}$ for Dy^{3+}, detected at 940 nm), showing rather good energy transfer efficiency from the ligand.[25]

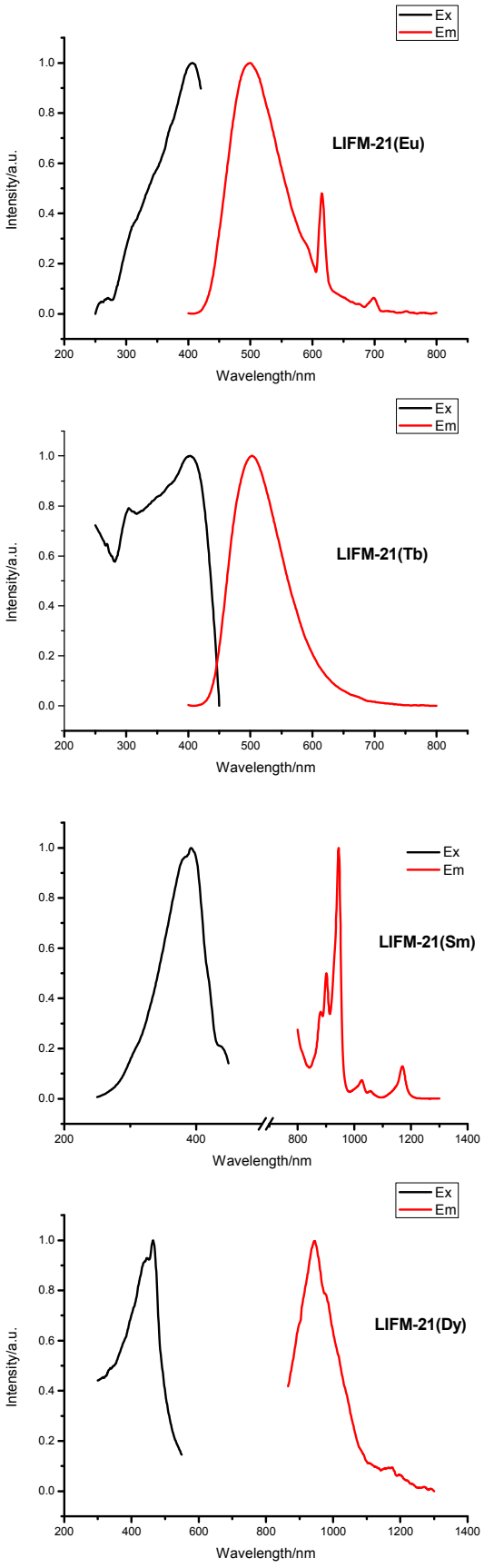

Fig. 5 Normalized excitation and emission spectra of LIFM-21(Eu, λ_{ex} = 397 nm, λ_{em} = 487 nm), LIFM-21(Tb, λ_{ex} = 395 nm, λ_{em} = 485 nm), LIFM-21(Sm, λ_{ex} = 395 nm, λ_{em} = 944 nm) and LIFM-21(Dy, λ_{ex} = 465 nm, λ_{em} = 829 nm).

Although complexes LIFM-21(Eu) and LIFM-21(Tb) do not represent good "antenna ligand" examples, the luminescence behaviour is still rather intriguing. Apart from the increased quantum yield observed in LIFM-21(Tb) described before, the two complexes also show solvofluorochromic phenomenon. As shown in Fig. 6, the emission of complex LIFM-21(Eu) in solution shows eye-detectable changes with the increase of the solvent polarity, spanning different colours from blue, cyan to green (Fig. 6a). Detailed luminescence spectra and calculated CIE coordinates (Figs. 6b and c) manifest the photophysical properties are simulateneously controlled by solubility/aggregate formation and solvent polarity. Genearlly, in good solvents such as DMF, methanol and DMSO, LIFM-21(Eu) is weakly emissive, similar to the situation in pure TPE-4PO ligand as discussed in Fig. 3. While in other relatively poor solvents, the emission colours of LIFM-21(Eu) are basically tuned by the solvent polarity monotonically. When dispersed in solvents with low polarity such as hexane, toluene and benzene, the emission colour of LIFM-21(Eu) is dark blue; in solvents with medium polarity such as *iso*-butyl acetate (*iso*-BA), ethyl acetate (EA), chloroform and dioxane, the emission colour becomes light blue to cyan; while in solvents with high polarity such as acetonitrile and glycol, the emission is further red-shifted to the green region. The fact that the weaken of solvent polarity will lead to energy rise (blue-shift) of the emission is also similar to that observed in the CH_2Cl_2/DMSO mixture solvent of TPE-4PO ligand, in which the ILCT emitting states are modified. The solvent responsive emission of LIFM-21(Tb) and pure TPE-4PO ligand show basically similar tendency (Figs. S6-7).

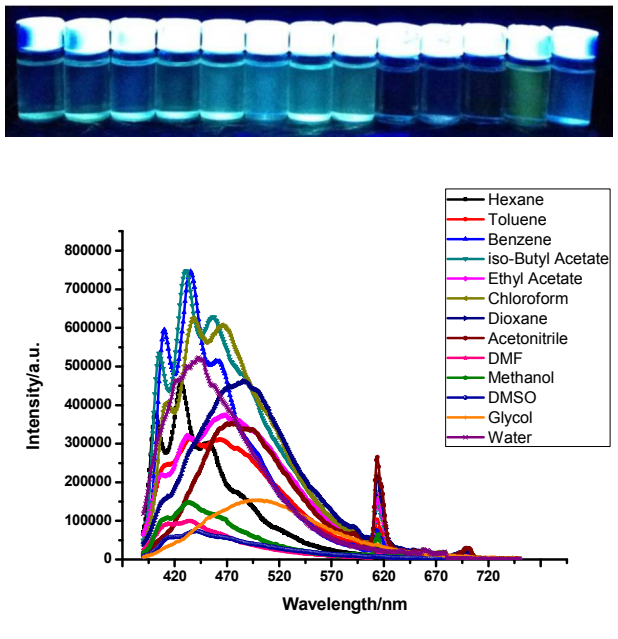

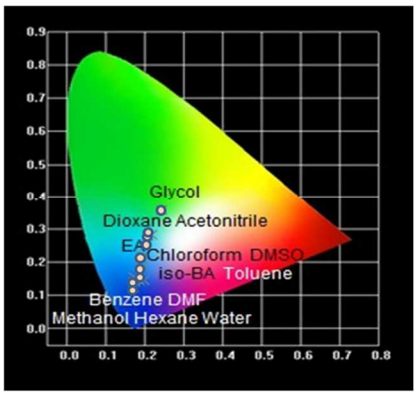

c)

Fig. 6 (a-c) Fluorescent photographs (in hexane, toluene, benzene, *iso*-butyl acetate, ethyl acetate, chloroform, dioxane, acetonitrile, DMF, methanol, DMSO, glycol, water, for which the polarities are increased steadily from left to right, respectively), emission spectra, and CIE coordinates of LIFM-21(Eu) dispersed in different solvents.

Conclusions

In general, a tetrapodal zwitterionic type ligand TPE-4PO was designed and applied to coordinate with Ln(III) ions Sm^{3+}, Eu^{3+}, Gd^{3+}, Tb^{3+}, Dy^{3+}. Both the ligand and lanthanide complexes show combined AIE/ILCT-dictated photoluminescence, which is multiple stimuli-responsive, including mechanofluorochromism, solvofluorochromism, and aggregation-inducive changes in the emission intensity and colors. Besides, the coordination with Tb^{3+} ions brings further rigidity to the TPE backbone, leading to intensified quantum efficiency. On the other hand, TPE-4PO can also serve as efficient antenna ligand to sensitize the NIR emission of Sm^{3+} and Dy^{3+}. Further studies on the application of this system for sensor devices and optoelectronic materials are undergoing.

Acknowledgements

This work was supported by 973 Program (2012CB821701), NSFC (91222201, 21373276), FRF for the Central Universities (15lgzd05), STPP of Guangzhou, and RFDPHE of China (20120171130006) for funding.

Notes and references

[a] MOE Laboratory of Bioinorganic and Synthetic Chemistry, State Key Laboratory of Optoelectronic Materials and Technologies, Lehn Institute of Functional Materials, School of Chemistry and Chemical Engineering, Sun Yat-Sen University, Guangzhou 510275, China
panm@mail.sysu.edu.cn; cesscy@mail.sysu.edu.cn

[b] State Key Laboratory of Structural Chemistry, Fujian Institute of Research on the Structure of Matter, Chinese Academy of Sciences, Fuzhou 350002, China

[c] State Key Laboratory of Organometallic Chemistry, Shanghai Institute of Organic Chemistry, Chinese Academy of Sciences, Shanghai 200032, China

Electronic Supplementary Information (ESI) available: [PXRD, TG, more luminescence spectra and crystallographic information]. See DOI: 10.1039/b000000x/

1. (*a*) J. Luo, Z. Xie, J. W. Y. Lam, L. Cheng, H. Chen, C. Qiu, H. S. Kwok, X. Zhan, Y. Liu, D. Zhu and B. Z. Tang, *Chem. Commun*., 2001, 1740; (*b*) B. Z. Tang, X. Zhan, G. Yu, P. P. S. Lee, Y. Liu and D. Zhu, *J. Mater. Chem.*, 2001, **11**, 2974; (*c*) Y. Hong, J. W. Y. Lam, B. Z. Tang, *Chem.Commun.*, 2009, 4332.
2. (*a*) C.-X. Yuan, X.-T. Tao, L. Wang, J.-X. Yang and M.-H. Jiang, *J. Phys. Chem. C*, 2009, **113**, 6809; (*b*) Y.-T. Wu, M.-Y. Kuo, Y.-T. Chang, C.-C. Shin, T.-C. Wu, C.-C. Tai, T.-H. Cheng and W.-S. Liu, *Angew. Chem., Int. Ed*., 2008, **120**, 10039; (*c*) C. J. Bhongale, C.-W. Chang, C.-S. Lee, E. W.-G. Diau, and C.-S. Hsu, *J. Phys. Chem. B*, 2005, **109**, 13472; (*d*) S. S. Palayangoda, X. Cai, R. M. Adhikari, and D. C. Neckers, *Org. Lett.*, 2008, **10**, 281; (*e*) H.-C. Yeh, W.-C. Wu, Y.-S. Wen, D.-C. Dai, J.-K. Wang, and C.-T. Chen, *J. Org. Chem.*, 2004, **69**, 6455.
3. (*a*) A. Y. Y. Tam, K. M. C. Wong, V. W. W. Yam, *J. Am. Chem.Soc.*, 2009, **131**, 6253; (*b*) M. X. Zhu, W. Lu, N. Zhu, C.-M. Che, *Chem.–Eur. J.*, 2008, **14**, 9736; (*c*) B. Manimaran, P. Thanasekaran, T. Rajendran, R.-J. Lin, I-J. Chang, G.-H. Lee, S.-M. Peng, S. Rajagopal, and K.-L. Lu, *Inorg. Chem.*, 2002, **41**, 5323; (*d*) Q. Zhao, L. Li, F. Li, M. Yu, Z. Liu, T. Yi and C. Huang, *Chem. Commun.*, 2008, 685.
4. (*a*) J. Zhang, Q. Yang, Y. Zhu, H. Liu, Z. Chi, C.-Y. Su, *Dalton Trans*., 2014, **43**, 15785; (*b*) H. Li, Y. Zhu, J. Zhang, Z. Chi, L. Chen, C.-Y Su, *RSC Adv.*, 2013, **3**, 16340; (*c*) J. Cheng, Y. Li, R. Sun, J. Liu, F. Gou, X. Zhou, H. Xiang, and J. Liu, *J. Mater. Chem. C*, 2015, DOI: 10.1039/C5TC02555A; (d) N. B. Shustova, T.-C. Ong, A. F. Cozzolino, V. K. Michaelis, R. G. Griffin, and M. Dincă, *J. Am. Chem. Soc.*, 2012, **134**, 15061.
5. (*a*) J. Liu, Y. Zhong, J. W. Y. Lam, P. Lu, Y. Hong, Y. Yu, Y. Yue, M. Faisal, H. H. Y. Sung, I. D. Williams, K. S. Wong and B. Z. Tang, *Macromolecules*, 2010, **43**, 4921; (*b*) W. Z. Yuan, P. Lu, S. Chen, J. W. Y. Lam, Z. Wang, Y. Liu, H. S. Kwok, Y. Ma, B. Z. Tang, *Adv. Mater.*, 2010, **22**, 2159.
6. (*a*) J. W. Chen, C. C. W. Law, J. W. Y. Lam, Y. P. Dong, S. M. F. Lo, I. D. Williams, D. B. Zhu and B. Z. Tang, *Chem. Mater.*, 2003, **15**, 1535; (*b*) Z. Li, Y. Q. Dong, B. X. Mi, Y. H. Tang, M. Häussler, H. Tong, Y. P. Dong, J. W. Y. Lam, Y. Ren, H. H. Y. Sung, K. S. Wong, P. Gao, I. D. Williams, H. S. Kwok and B. Z. Tang, *J. Phys. Chem. B*, 2005, **109**, 10061.
7. (*a*) J. Wang, J. Mei, R. Hu, J. Z. Sun, A. Qin and B. Z. Tang, *J. Am. Chem. Soc.*, 2012, **134**, 9956; (*b*) N. Zhao, Z. Y. Yang, J. W. Y. Lam, H. H. Y. Sung, N. Xie, S. J. Chen, H. M. Su, M. Gao, I. D. Williams, K. S. Wong and B. Z. Tang, *Chem. Commun.*, 2012, **48**, 8637; (*c*) Q. Zhang, J. Su, D. Feng, Z. Wei, X. Zou, H.-C. Zhou, *J. Am, Chem. Soc.*, 2015, **134**, 10064–10067.
8. (*a*) Q. Qi, Y. Liu, X. Fang, Y. Zhang, P. Chen, Y. Wang, B. Yang, B. Xu, W. Tian and S. X.-A. Zhang, *RSC Adv.*, 2013, **3**, 7996; (*b*) Z. Chi, X. Zhang, B. Xu, X. Zhou, C. Ma, Y. Zhang, S. Liu and J. Xu, *Chem.*

Soc. Rev., 2012, **41**, 3878.

9. (*a*) S. J. Toal, K. A. Jones, D. Magde and W. C. Trogler, *J. Am. Chem. Soc.*, 2005, **127**, 11661; (*b*) M. Kinami, B. R. Crenshaw and C. Weder, *Chem. Mater.*, 2006, **18**, 946; (*c*) B. R. Crenshaw, M. Burnworth, D. Khariwala, A. Hiltner, P. T. Mather, R. Simha and C. Weder, *Macromolecules*, 2007, **40**, 2400.
10. (*a*) M. Irie, T. Fukaminato, T. Sasaki, N. Tamai and T. Kawai, *Nature*, 2002, **420**, 759; (*b*) C. E. Olson, M. J. R. Previte and J. T. Fourkas, *Nat. Mater.*, 2002, **1**, 225; (*c*) S. J. Lim, B. K. An, S. D. Jung, M. A. Chung and S. Y. Park, *Angew. Chem., Int. Ed.*, 2004, **43**, 6346; (*d*) S. Hirata and T. Watanabe, *Adv. Mater.*, 2006, **18**, 2725.
11. A. Kishimura, T. Yamashita, K. Yamaguchi and T. Aida, *Nat. Mater.*, 2005, **4**, 546.
12. (*a*) N. Mizoshita, T. Tani and S. Inagaki, *Adv. Mater.*, 2012, **24**, 3350; (*b)* S. J. Yoon, J. W. Chung, J. Gierschner, K. S. Kim, M. G. Choi, D. Kim and S. Y. Park, *J. Am. Chem. Soc*., 2010, **132**, 13675.
13. (*a*) Y. Dong, B. Xu, J. Zhang, X. Tan, L. Wang, J. Chen, H. Lv, S. Wen, B. Li, L. Ye, B. Zou and W. Tian, *Angew. Chem., Int. Ed.*, 2012, **51**, 10782; (*b*) F. Chen, J. Zhang and X. Wan, *Chem.–Eur. J*., 2012, **18**, 4558.
14. (*a*) Z. R. Grabowski, K. Rotkiewicz, W. Rettig, *Chem. Rev.*, 2003, **103**, 3899; (*b*) C. E. Powell, M. G. Humphrey, *Coord. Chem. Rev.*, 2004, **248**, 725; (*c*) O. Maury, H. Le Bozec, *Acc. Chem. Res.*, 2005, **38**, 691; (*d*) G. S. He, L.-S. Tan, Q. Zheng, P. N. Prasad, *Chem. Rev.*, 2008, **108**, 1245.
15. (*a*) M. K. Kuimova, G. Yahioglu, J. A. Levitt, K. Suhling, *J. Am. Chem. Soc.*, 2008, **130**, 6672; (*b*) M. Pawlicki, H. A. Collins, R. G. Denning, H. L. Anderson, *Angew. Chem. Int. Ed.*, 2009, **48**, 3244.
16. (*a*) H. M. Kim, B. R. Cho, *Chem. Commun.*, 2009, 153; (*b*) M.A. Haidekker, T.P. Brady, D. Lichlyter, E.A. Theodorakis, *J. Am. Chem. Soc.*, 2006, **128**, 398.
17. (*a*) Q. Y. Yang, J. M. Lehn, *Angew. Chem. Int. Ed.*, 2014, **126**, 4660; (*b*) B.-B. Du, Y.-X. Zhu, M. Pan, M.-Q. Yue, Y.-J. Hou, K. Wu, L.-Y. Zhang, L. Chen, S.-Y. Yin, Y.-N. Fan, and C.-Y. Su, *Chem. Commun*, 2015, **51**, 12533; (*c*) Q.-Y. Yang, K. Wu, J.-J. Jiang, C.-W. Hsu, M. Pan, J.-M. Lehn and C.-Y. Su, *Chem. Commun.*, 2014, **50**, 7702; (*d*) Q.-Y. Yang, M. Pan, S.-C. Wei, K. Li, B.-B. Du, C.-Y Su, *Inorg. Chem.*, 2015, **54,** 5707.
18. (*a*) A. Qin, J. W. Y. Lam, L.Tang, C. K. W. Jim, H. Zhao, J. Sun and B. Z. Tang, *Macromolecules*, 2009, **42**, 1421; (*b*) M. Wang, X. Gu, G. Zhang, D. Zhang and D. Zhu, *Anal. Chem.*, 2009, **81**, 4444; (*c*) S. Jayanty, T. P. Radhakrishnan, *Chem.–Eur. J.*, 2004, **10**, 791
19. (*a*) S. J. Toal, K. A. Jones, D. Magde, and W. C. Trogler, J. *Am. Chem. Soc.*, 2005, **127**, 11661; (*b*) F. Mahtab, Y. Yu, J. W. Y. Lam, J. Liu, B. Zhang, P. Lu, X. Zhang, B. Z. Tang, *Adv. Funct. Mater.*, 2011, **21**, 1733.
20. G. Sheldrick, "SHELXL-2013", 2013, Universität Göttingen, Göttingen, Germany.
21. T. S. Navale, K. Thakur, R. Rathore, *Org. lett.*, 2011, **13**, 1634.
22. X. Yan, T. R. Cook, P. Wang, F. Huang and P. J. Stang, *Nat. Chem.*, 2015, **7**, 342.
23. (*a*) C. Bazzicalupi, A. Bencini, A. Bianchi, C. Giorgi, V. Fusi, A. Masotti, B. Valtancoli, A. Roque, F. Pina, *Chem. Commun.*, 2000, **7**, 561; (*b*) S. V. Eliseeva and J.-C. G. Bünzli, *Chem. Soc. Rev.*, 2010, **39**, 189; (*c*) M. Latva, H. Takalo, V.-M. Mukkala, C. Matachescu, J. C. Rodríguez-Ubis, J. Kankare, *J. Lumin.*, 1997, **75**, 149 .
24. Z. Wei, Z.-Y. Gu, R. K. Arvapally, Y.-P. Chen, R. N. McDougald, J. F. Ivy A. A. Yakovenko, D. Feng, M. A. Omary, and H.-C. Zhou, *J. Am. Chem. Soc.*, 2014, **136**, 8269.
25. (*a*) A. Foucault-Collet, C. M. Shade, I. Nazarenko, S. Petoud, S. V. Eliseeva, *Angew. Chem. Int. Ed.*, 2014, **53**, 2927; (*b*) L. Sun, Z. Wang, J. Z. Zhang, J. Feng, J. Liu, Y. Zhao, L. Shi, *RSC Adv.,* 2014, **4**, 28481; (*c*) S. Biju, Y. K. Eom, J.-C. G. Bünzli, H. K. Kim, *J. Mater. Chem. C*, 2013, **1**, 6935; (*d*) Q.-Y. Yang, M. Pan, S.-C. Wei, C.-W. Hsu, J.-M Lehn, C.-Y. Su, *CrystEngComm*, 2014, **16**, 6469; (e) T. D. Pasatoiu, C. Tiseanu, A. M. Madalan, B. Jurca, C. Duhayon, J. Pascal Sutter, and M.Andruh, *Inorg. chem*., 2011, **50**, 5879.

Table of contents entry

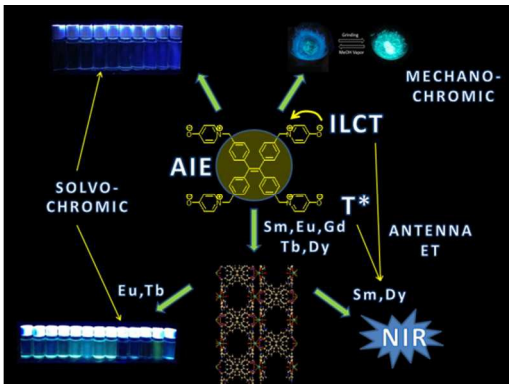

AIE and ILCT properties are combined in one zwitterionic-type ligand and its assembled lanthanide complexes.